



Supporting Online Material for

A Cretaceous Scleractinian Coral with a Calcitic Skeleton

Jarosław Stolarski,* Anders Meibom, Radosław Przeniosło, Maciej Mazur

*To whom correspondence should be addressed. E-mail: stolacy@twarda.pan.pl

Published 5 October 2007, *Science* **318**, 92 (2007)

DOI: 10.1126/science.1149237

This PDF file includes:

Materials and Methods
Figs. S1 to S7
References

Supporting Online Material for

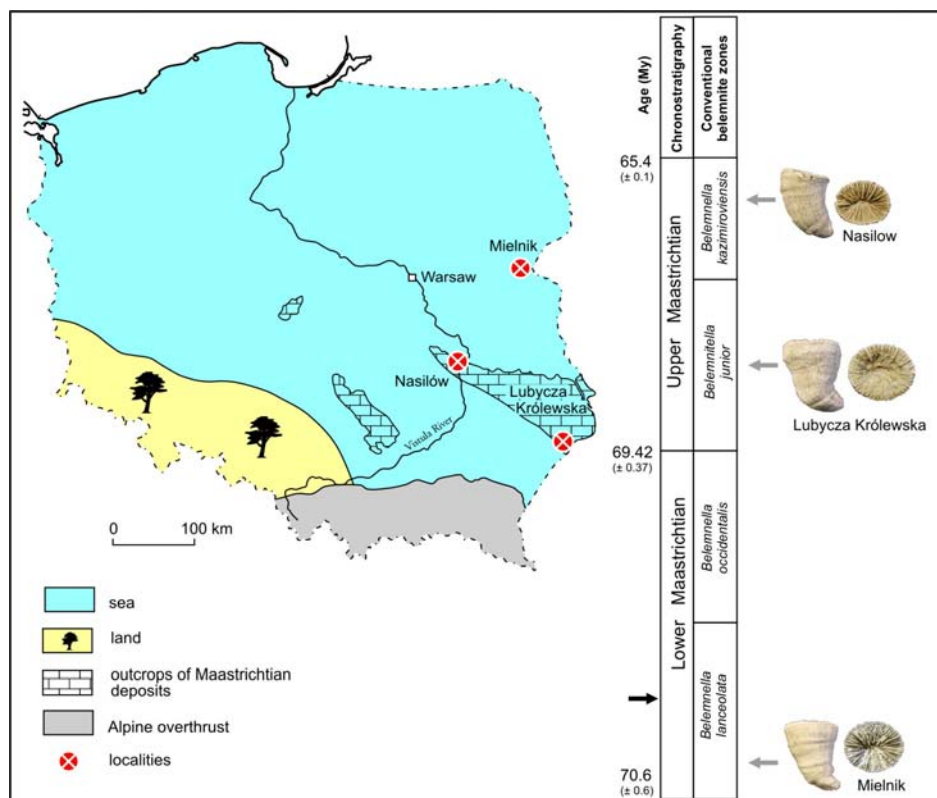
A Cretaceous Scleractinian Coral with a Calcitic Skeleton

Jarosław Stolarski*, Anders Meibom, Radosław Przeniosło & Maciej Mazur

* To whom correspondence should be addressed. E-mail: stolacy@twarda.pan.pl

Materials

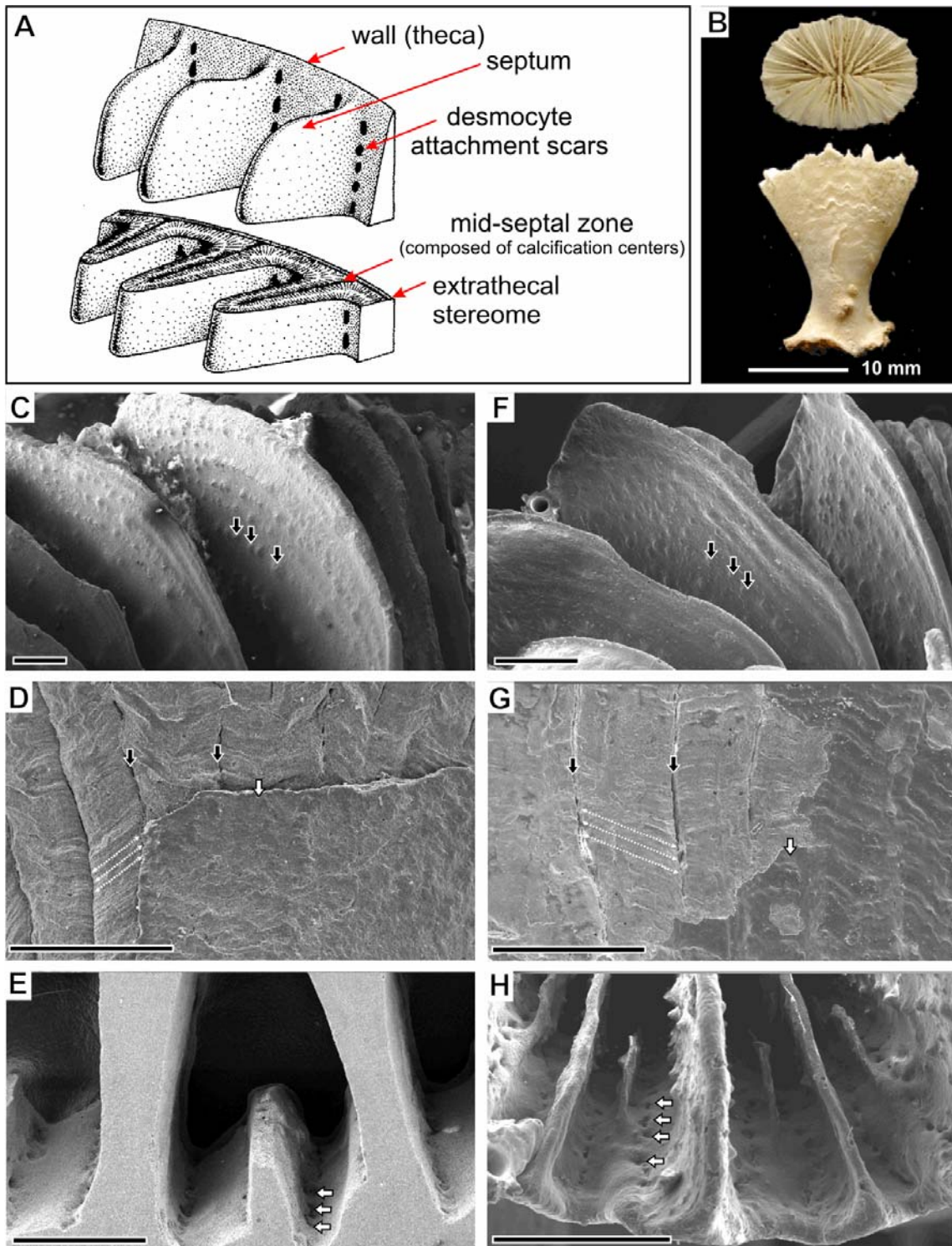
LOCALITIES. The examined specimens of *Coelosmilia* sp. are from the Upper Cretaceous (Maastrichtian) sediments of Poland. These mostly carbonate deposits, locally with siliciclastic input, are part of the larger marine epicratonic sequence formed in the Late Cretaceous between the mid-European island to the south and Baltic Shield to the north (1). The *Coelosmilia* sp. specimens studied here are from the Maastrichtian sediments exposed in three localities (Suppl-Fig. 1): Nasiłów (Middle Vistula Valley section, central Poland), Lubycza Królewska (Lublin Upland, SE Poland), and Mielnik (Eastern Poland). Samples from the Mielnik chalk-pit have been collected from the Lower Maastrichtian part (*Belemnella lanceolata* Zone) of the Campanian-Maastrichtian mid- to outershelf white chalk succession (2). Corals from Lubycza Królewska are from the natural exposure of the lower Upper Maastrichtian (*Belemnitella junior* Zone) marly-siliceous limestones (3) representing mid- to outershelf settings and those of Nasiłów quarry are from the bottom of the upper Upper Maastrichtian (*Belemnella kazimiroviensis* Zone) inner-shelf marly-siliceous limestones (4,5).



Supp-Fig. 1. Simplified paleogeography of Poland in Maastrichtian, Late Cretaceous (6). Location and approximate stratigraphic position of the *Coelosmilia* sp. finds in the Mielnik, Nasiłów and Lubycza Królewska localities are indicated. Black arrow on the left of the conventional belemnite zonation column indicates the new, recently suggested Early/Late Maastrichtian boundary (7, 8).

SPECIMENS. Coralla of *Coelosmilia* sp. are solitary with ceratoid, typically curved base in the plane of shorter calicular axis. The proximal part forms a short pedicel. Calice is elliptical (up to 35 x 31 mm) and about 36 mm in height. Costae form low ridges, more distinct for primary septa. Costae are covered with thin extra-theal stereome (tectura) decorated with small, rounded granules (Suppl-Fig. 2C). Septa are arranged in 5 full septal cycles (96 septa) that are differentiated into 3 distinct size classes of decreasing 'exertness': 24 moderately exert S1-S3, 24 less exert S4, and 48 small S5 septa. Regularly distributed shallow pits of desmocyte attachment scars occur occasionally on the inner wall surface at the base of septa (Suppl-Fig. 2E). Calicular depression (fossa) is deep (ca. 10 mm) and larger septa fuse at its bottom to form rudimentary columella. Lower in the calice, spaces between neighboring septa are often filled completely with stereome. The described species are most similar to *C. cornucopiae* (Duncan, 1869) (9).

Specimen identification numbers: Cretaceous *Coelosmilia* sp. from Lubycza Królewska: ZPAL H.II/6; from Mielnik: ZPAL H.II/8; from Nasiłów: ZPAL H.II/7. Recent *Desmophyllum* sp. from Pacific Ocean, 51⁰52,0'S/73⁰41,0'W and 636 m: ZPAL H.25/5; *Javania* sp. from Indian Ocean, 12⁰43,7'N/43⁰15,0'E and 228–235 m: ZPAL H.25/6.

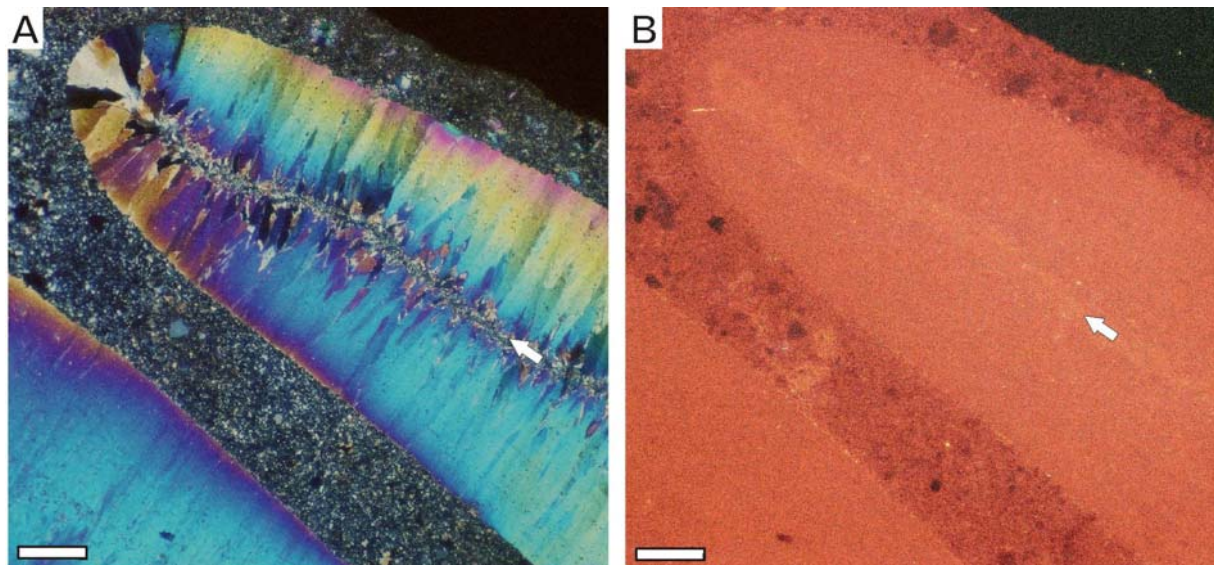


Supp-Fig. 2. Micro-architectural details of the Cretaceous, calcitic skeleton of *Coelosmia* sp. (left column, C-E) in direct comparison with the modern, aragonitic skeleton of *Javania* sp. (right column, F-H). (A) Schematic drawing of a corallum fragment (transverse section) with main structural characters explained. (B) Corallum of *Javania* sp. in distal (upper image) and lateral (lower image) views. (C, F) Septal faces covered with rows of fine granulations (arrows). (D, G) External surface of the wall with extrathecal stereome (white arrow) partly removed: mid-septal zones are exposed (black arrows) and growth lines of the marginothecal wall (10) are clearly visible (white dashed lines). (E, H) rows of desmocyte attachment scars (arrows) mark sites at which the polyp was attached to the skeleton (11). Scale-bar is 1 mm unless otherwise noted.

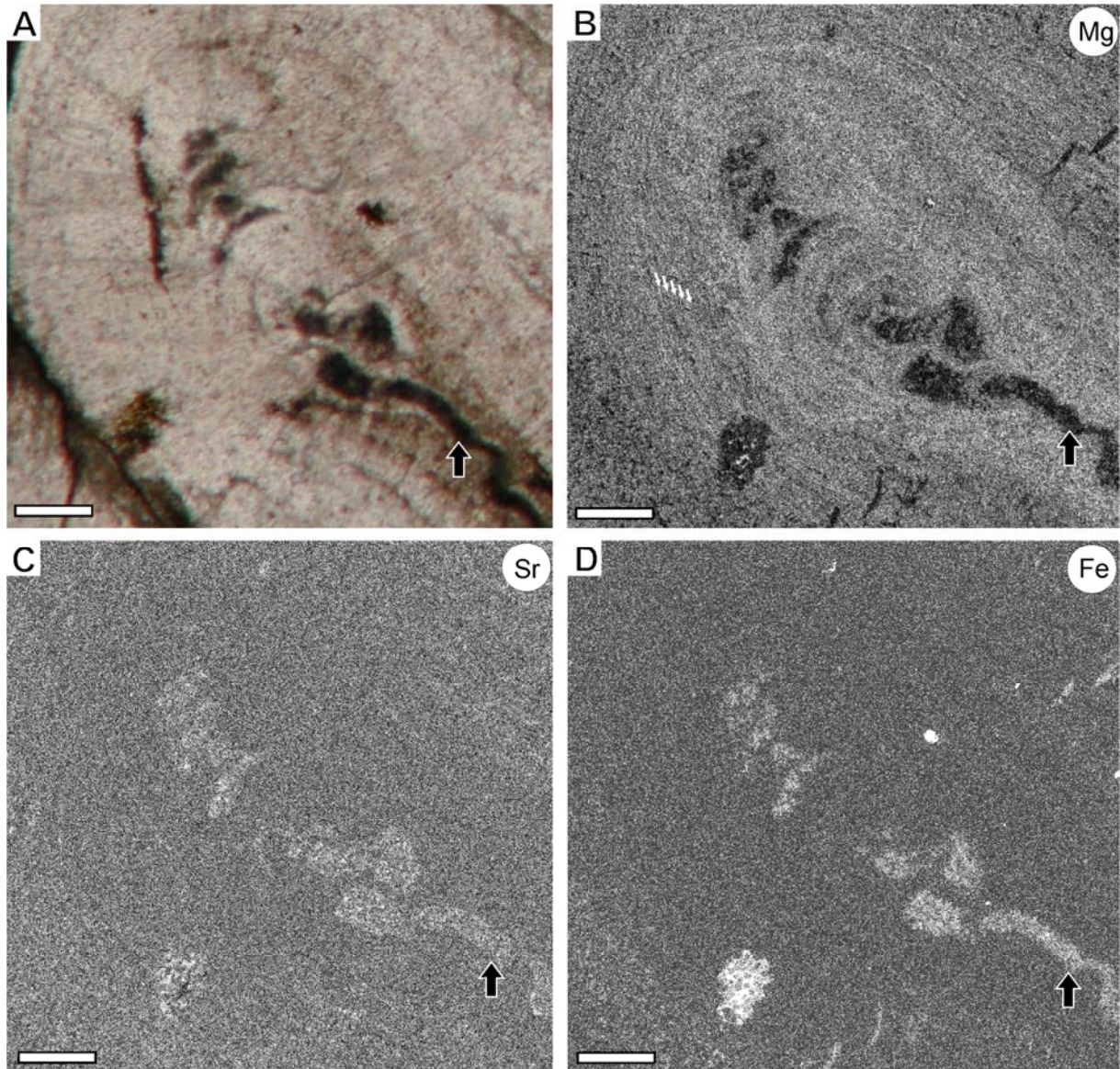
CATHODOLUMINESCENCE, WAVELENGTH DISPERSIVE SPECTROSCOPY (WDS) ELEMENTAL MAPPINGS AND MOLECULAR FLUORESCENCE OBSERVATIONS.

Cathodoluminescence observations and WDS elemental mappings provide evidence for some diagenetic changes in the mid-septal region, but show that structure of the fibrous skeleton is unaffected by diagenesis (Suppl-Figs. 3, 4). The mid-septal zone is enriched in iron minerals (Suppl-Fig. 4D). Fe-enriched spots (depleted in Mg) occur occasionally also outside the mid-septal zone but they are invariably associated with fractures and mechanical damages of the skeleton. In modern corals, mid-septal region (calcification centers) is composed mostly of organic components that are the first to decay and to be removed from the skeleton after burial. Regions rich in organics can be selectively removed by endolithic microorganisms associated with iron-manganese precipitating bacteria (12). As a rule, organic components from the mid-septal zone are not preserved in fossil corals but frequently their original fine-scale arrangement is still recognizable because of perfect replacement by the secondary minerals. Dimensions and arrangement of trabecular rods within the mid-septal zone support this interpretation for *Coelosmilia* sp. skeleton. On the other hand, micro-zonation in Mg concentration within fibrous skeleton (Suppl-Fig. 4B) supports its original microstructural organization. Although spatial resolution of WDS mappings is less accurate than high spatial resolution secondary ion mass spectrometry (NanoSIMS) mappings, micro-zonation and increasingly higher Mg concentrations towards the region of the former mid-septal zone are fully comparable with zonal pattern of Mg distribution in modern corals (13).

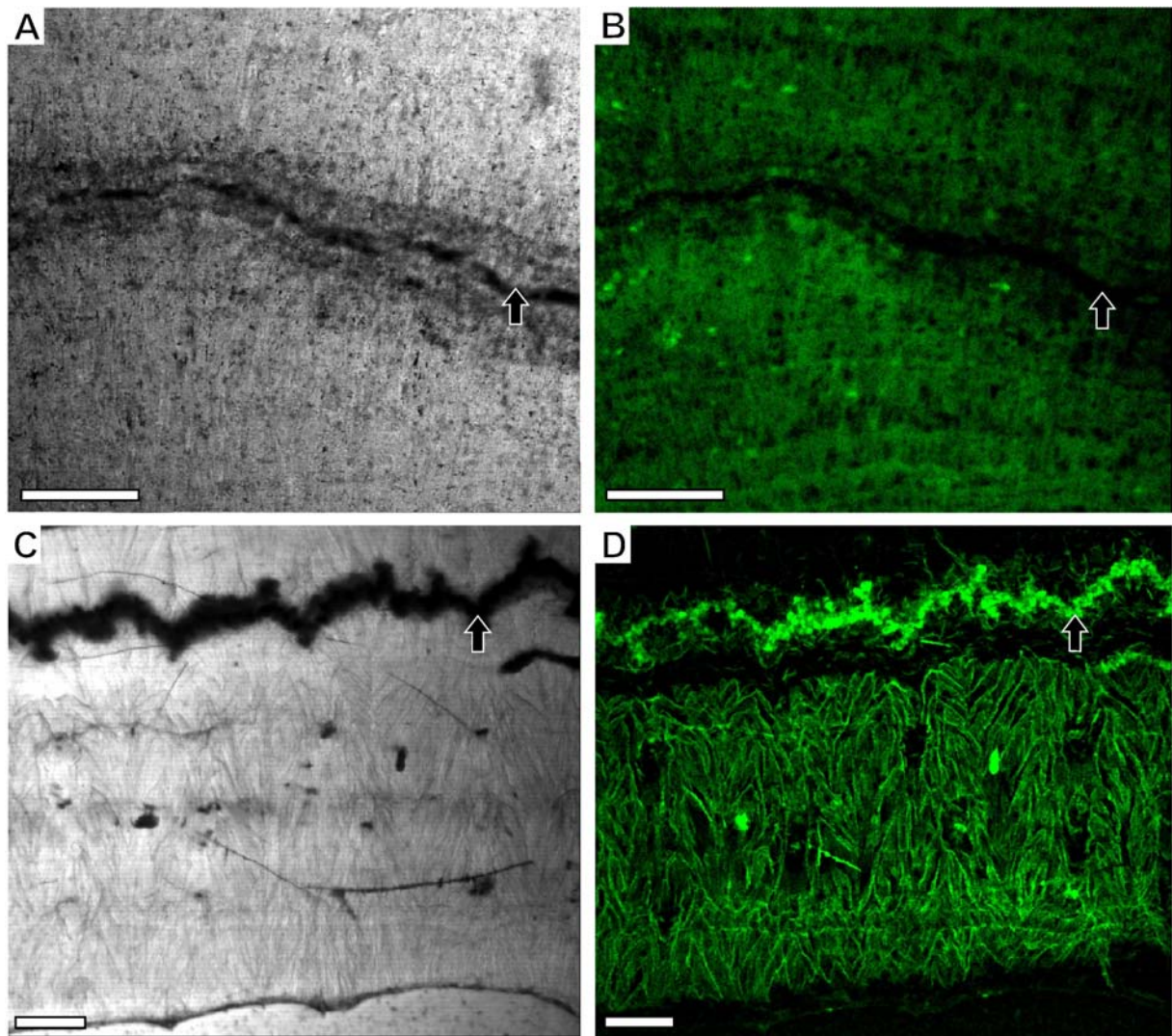
Although the bulk of organic components (mid-septal zone) has been removed from the skeleton of *Coelosmilia* sp., organics trapped within the fibrous part are visible on images from the confocal scanning fluorescent microscopy. Fluorescence response is less intense in comparison with modern corals (Suppl-Fig. 5D), however concentration of intra-skeletal organic components occur along the successive layers and radial "envelopes" of the fiber bundles (Suppl-Fig. 5B). Lack of organic components within mid-septal zone of *Coelosmilia* sp. is consistent with geochemical WDS mappings.



Supp-Fig. 3. Transverse section of septum in the Cretaceous, calcitic *Coelosmilia* sp. photographed by optical microscopy (A) and by cathodoluminescence microscopy (B). Brighter luminescence of the mid-septal zone (arrow) suggests some diagenetic alteration of this region (confirmed by WDS mappings); in contrast, the absence of cloudy luminescence in the fibrous part indicate that major recrystallization did not take place. Scale bar is 100 μ m.



Supp-Fig. 4. Transversely sectioned septum of the Cretaceous, calcitic *Coelosmilia* sp. in optical microscope (A) and distribution of Magnesium (B), Strontium (C) and Iron (D) mapped with Wavelength Dispersive Spectroscopy technique. The mid-septal zone (black arrows) is enriched in iron minerals. In modern corals, mid-septal region (calcification centers) is composed mostly of organic components that are the first to decay and to be removed from the skeleton after burial. As a rule, organics from mid-septal zone is not preserved in fossil corals¹⁵ and early diagenetic replacement with iron minerals has been reported also from modern corals¹². The layered structure of the "fibrous" skeleton is highlighted by micro-scale zoning in Mg concentration (B, small white arrows), similarly as in modern corals¹³. Scale-bar is 100 μ m.



Supp-Fig. 5. Transversely sectioned septum of the Cretaceous, calcitic *Coelosmilia* sp. (A,B) and Recent, aragonitic *Desmophyllum* sp. (C,D) in optical (A,C) and laser confocal scanning fluorescent microscopes (B, D). Organic components stained with acridine orange are visible in skeletal regions of *Desmophyllum* sp. septum: mid-septal zone (D, black arrow) and as "organic envelopes" in fibrous part. Although in *Coelosmilia* sp. mid-septal zone lacks organic components (result consistent with geochemical mapping, Supp-Fig. 3) there is clear fluorescence response in the fibrous skeleton (B). Scale-bar is 100 μm .

Methods

Trace element analyses were performed with the Cameca NanoSIMS N50 at the Muséum National d'Histoire Naturelle in Paris, following established procedures (13, 15). Briefly, septa were cut perpendicular to their growth direction, mounted in epoxy (Körpox©) and polished to a 0.25 μm finish using diamond paste. The samples were then gold-coated. Using a primary beam of O^- , secondary ions of $^{24}\text{Mg}^+$, $^{44}\text{Ca}^+$ and $^{88}\text{Sr}^+$ were sputtered from the sample surface and detected simultaneously (multicollection-mode) in electron-multipliers at a mass-resolving power of ~ 4500 ($M/\Delta M$). At this mass-resolving power, the measured secondary ions are resolved from potential interferences. Data were obtained from a pre-sputtered surface in a series of line-scans with the primary ions focused to a spot-size of ~ 200 nm and the primary beam was stepped across the sample surface with a similar step-size. The measured $^{24}\text{Mg}/^{44}\text{Ca}$ and $^{88}\text{Sr}/^{44}\text{Ca}$ ratios were calibrated against analyses of carbonate standards of known composition. The chemical variations recorded in the coral skeletons are

much larger than both the internal and external reproducibility of the standards, which are typically <10% for Mg/Ca and <5% for Sr/Ca.

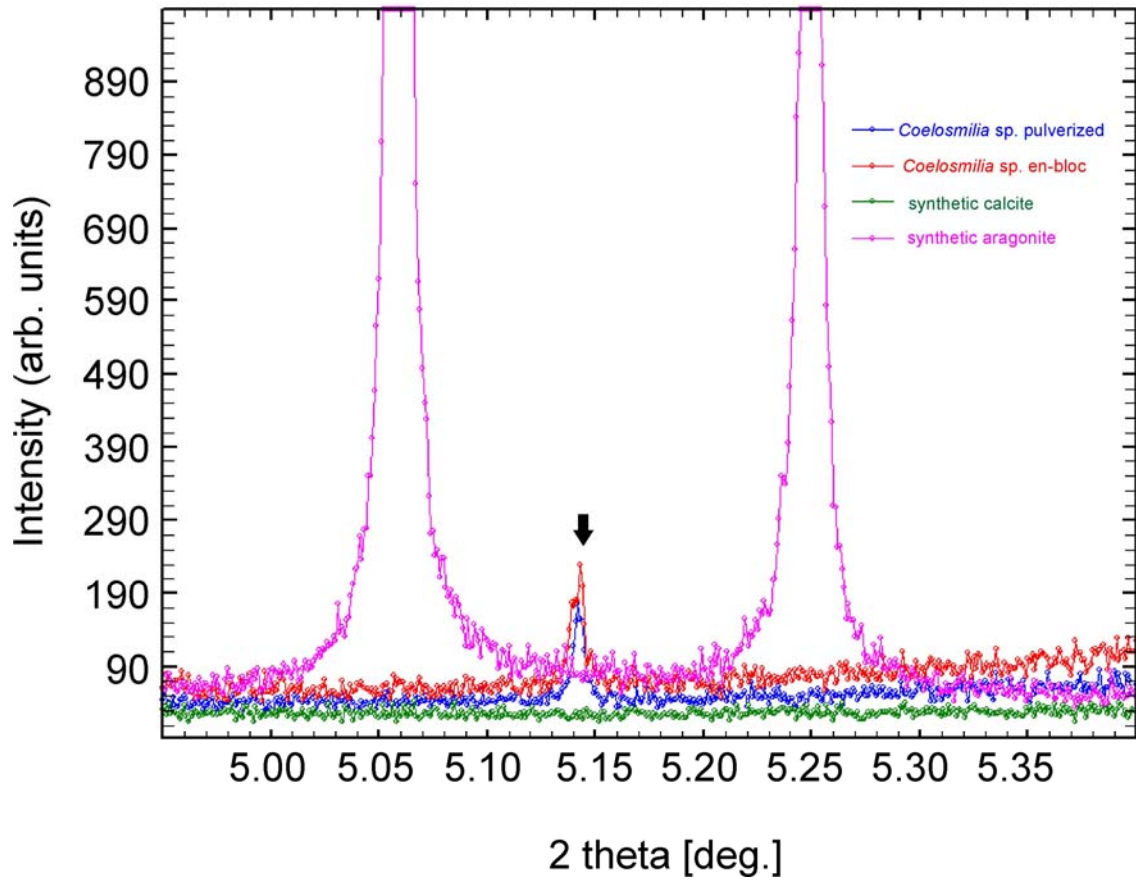
Atomic Force Microscopy was performed with a MultiMode Nanoscope IIIa (Digital Instruments, Veeco), following described procedures (14). Standard silicone nitride cantilevers were used for measurements in contact mode. The coral samples consist of septa cut transversal to their growth direction, were polished with diamond suspension of grain sizes 5 and 1 micrometers, and then with aluminium oxide (Buehler TOPOL 3 final polishing suspension with particle size 0.25 micrometers). After polishing, the sections were rinsed in Milli-Q water and washed in an ultrasonic cleaner for 10 seconds. The polished samples were then etched in 1% ammonium persulfate in McIlvain buffer (pH=8) for 10 min, followed by rinsing in deionized water and drying.

Polished thin sections were examined with a Cambridge CCL Cold Cathodoluminescence 8200 mk3 system mounted on Nikon Optiphot 2 microscope at the Polish Geological Institute in Warsaw (Dr M. Sikorska-Jaworowska lab).

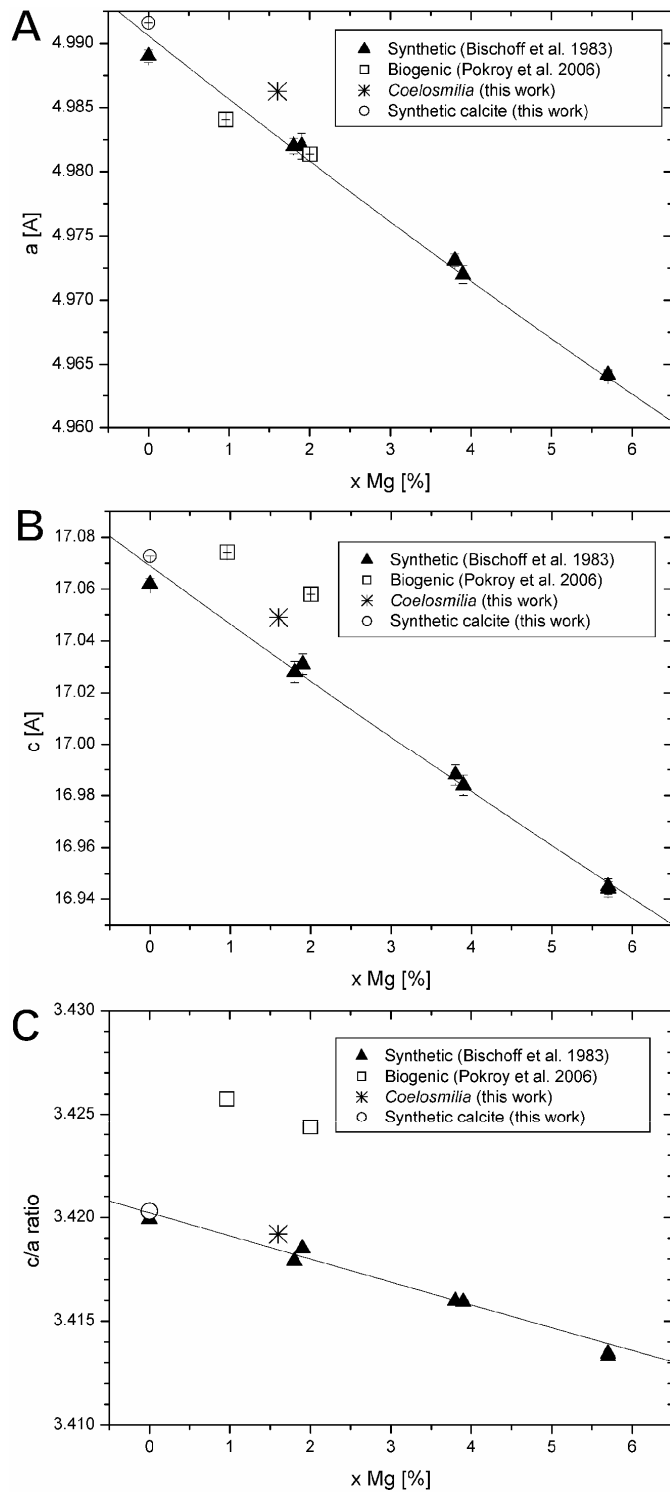
Wavelength Dispersive Spectroscopy elemental X-ray mapping were acquired on a Cameca SX-100 electron microprobe at the Inter-Institute Analytical Complex for Minerals and Synthetic Substances, Electron Microprobe Laboratory (Department of Geology, Warsaw University) using described procedures (10). The following conditions were used during stage scan: 15 kV (accelerating voltage), 20 nA (beam current), 60msek (pixel time), and ca. 1 μm spacing (515 x 515 pixel resolution). Specimens were coated with platinum of ca. 2nm thickness.

Laser Confocal Scanning Fluorescence Microscope observations sections were acquired on a Leica TCS SP1 Confocal Microscope at the Natural History Museum, London (GB-TAF-2213 Synthesis of Systematic Resources EU Program). Following described preparative procedures (16), polished sections were stained in a 0.45 μm filtered 1% acridine orange aqueous solution for 5 minutes. Stained samples were briefly rinsed in distilled water and air dried.

Synchrotron radiation high resolution powder diffraction measurements were performed at the beamline ID31 at ESRF Grenoble, on both pulverized samples and samples extracted *en-bloc*, following described procedures (17). The beamsize was approximately rectangular 1 mm by 3 mm and the illuminated sample thickness is about 3mm. Measured wavelength value was refined from measurements with a Si sample (NIST standard). The diffractometer resolution was estimated from measurements with LaB₆ and wavelength used during measurement was 0.30020(4) Å. The synthetic calcite was a commercial sample provided by Sigma-Aldrich (product code: C4830). The reference geological aragonite came from Tazouta Mine in the Atlas Mountains, Morocco (Sefrou, Sefrou Prefecture, Fès-Boulemane Region). Diffraction pattern of *Coelosmilia* sp. skeleton was compared against the calcite (18) and aragonite (19) crystal structure. Pulverized skeleton of *Coelosmilia* sp., modern *Desmophyllum* sp. and reference aragonite and calcite samples were sealed in borosilicate capillaries 0.7 mm in diameter; illuminated volume ca. 1.1 mm³. Measurements were also performed on several *Coelosmilia* sp. samples extracted *en-bloc*; illuminated volume ca. 9 mm³ for each sample (Suppl-Fig. 5). Structural parameters of examined calcite samples have been refined from their diffraction patterns by using the Rietveld method (20). These results were compared with synthetic (21) and biogenic (22) Mg-containing calcite samples (Suppl-Fig. 6).



Supp-Fig. 6. Enlarged part of the SR diffraction pattern of reference aragonite (purple line), synthetic calcite (green line), *en-bloc* (red line) and pulverized (blue line) *Coelosmilia* sp. specimen. The weak single Bragg peak at $2\theta = 5.140$ deg. (black arrow) is due to a minor quartz impurity (0.25%) phase (23). The main Bragg peaks due to aragonite located at $2\theta = 5.0578$ and 5.2494 deg. are absent in the *Coelosmilia* sp. SR diffraction pattern.



Supp-Fig. 7. Calcite lattice parameters a (A), c (B) and their ratio c/a (C) as a function of Mg content x [%]. The solid lines show the $a(x)$, $c(x)$ and $c(x)/a(x)$ quadratic functions refined for synthetic Mg doped calcite (21, solid triangles). Open squares show results from biogenic calcite (22). Our results for *Coelosmilia* sp. (star). Our reference synthetic calcite (open circle). Both a and c lattice parameters obtained for *Coelosmilia* sp. are larger than the corresponding synthetic calcite with the same Mg content (about 1.6%).

References:

- S1. W. K. Christensen, *Palaeont. Z.* **60**, 113–129 (1976).
- S2. D. Olszewska, *Acta Geol. Pol.* **40**, 111–128 (1990).
- S3. S. Cieśliński, J. Rzechowski, *Tektonika Roztocza i jej aspekty sedymentologiczne, hydrologiczne i geomorfologiczno–krajobrazowe* (Towarzystwo Wolnej Wszechnicy Polskiej, Lublin, 1993), pp. 38–46.
- S4. G. I. Abdel–Gawad, *Acta Geol. Pol.* **36**, 69–224 (1986).
- S5. M. Machalski, *Cretaceous Res.* **26**, 813–836 (2005).
- S6. J. Świdrowska, M. Hakenberg, *Przegląd Geologiczny* **47**, 61–68 (1999).
- S7. J. W. M. Jagt, W. J. Kennedy, *Neues Jahrb. Geol. P- M.* **4**, 239–245 (1994).
- S8. G. S. Odin, M. A. Lamaurelle, *Episodes* **4**, 229–238 (2001).
- S9. P. M. Duncan, *Palaeontographical Society Monographs, London* 1–44 (1869).
- S10. J. Stolarski, *Acta Palaeontol. Pol.* **40**, 19–44 (1995).
- S11. S. W. Wise, *Science* **169**, 978–980 (1970).
- S12. J. Sorauf, A. Freiwald, *Coral Res. Bull.* **7**, 191–207 (2002).
- S13. A. Meibom, J. P. Cuif, F. Hillion, B. R. Constantz, A. Juillet-Leclerc, Y. Dauphin, T. Watanabe, R. B. Dunbar, *Geophys. Res. Lett.* **31**, L23306, doi:10.1029/2004GL021313 (2004).
- S14. J. Stolarski, M. Mazur, *Acta Palaeontol. Pol.* **50**, 847–865 (2005).
- S15. A. Meibom, S. Mostefaoui, J. P. Cuif, Y. Dauphin, F. Houlbreque, R. Dunbar, B. Constantz, *Geophys. Res. Lett.* **34**, L02601, doi:10.1029/2006GL028657 (2007).
- S16. J. Stolarski, *Acta Palaeontol. Pol.* **48**, 497–530 (2003).
- S17. J. Stolarski, R. Przeniosło, M. Mazur, M. Brunelli, *J. Appl. Crystallogr.* **40**, 2–9 (2007).
- S18. E. N. Maslen, V. A. Streltsov, N. R. Streltsova, N. Ishizawa, *Acta Crystallogr. B* **51**, 929–939 (1995).
- S19. E. N. Caspi, B. Pokroy, P. L. Lee, J. P. Quintana, E. Zolotoyabko, *Acta Crystallogr. B* **61**, 129–132 (2005).
- S20. J. Rodriguez-Carvajal, *Physica B* **192**, 55–69 (1993).
- S21. W.D. Bischoff, F.C. Bishop, F.T. Mackenzie, *Am. Mineral.* **68**, 1183–1188 (1983).
- S22. B. Pokroy, A. N. Fitch, F. Marin, M. Kapon, N. Adir, E. Zolotoyabko, *J. Struct. Biol.* **155**, 96–103 (2006).
- S23. J. Jorgensen, *J. Appl. Phys.* **49**, 5473–5478 (1978).